Colloids and Surfaces A: Physicochemical and Engineering Aspects 681 (2024) 132828

Contents lists available at ScienceDirect

Colloids and Surfaces A: Physicochemical and Engineering Aspects

journal homepage: www.elsevier.com/locate/colsurfa

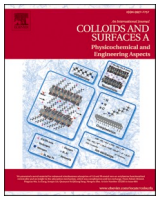

Surface and foam properties of polyvinyl alcohol solutions

V. Georgiev [a], Z. Mitrinova [a], N. Genchev [a], Alexander Gers-Barlag [b], Guillaume Jaunky [b], N. Denkov [a], S. Tcholakova [a,*]

[a] Department of Chemical Engineering, Sofia University, Sofia, Bulgaria
[b] BYK Chemie, Germany

GRAPHICAL ABSTRACT

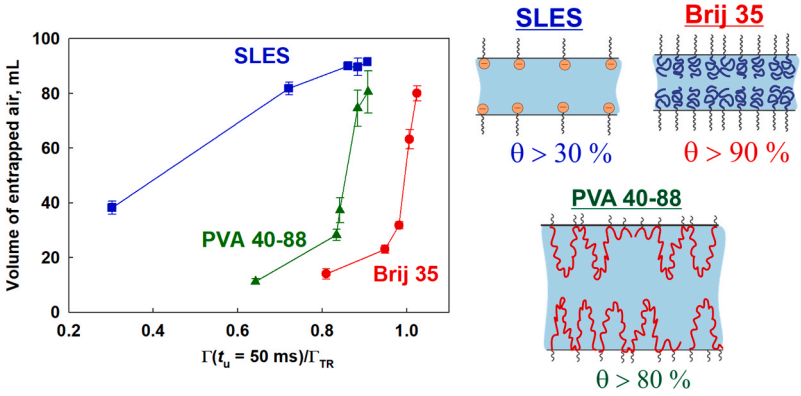

ARTICLE INFO

Keywords:
Foams
Polyvinyl alcohol
Surface coverage
Bartsch test
Foam rise method
Degree of hydrolysis

ABSTRACT

The surface, film, and foam properties of six polyvinyl alcohols (PVA) with different degrees of hydrolysis (DH) and molecular weights were studied and compared with the properties of nonionic Brij 35 and anionic SLES. Four different foaming methods were employed: the fast foaming method (Bartsch test), intermediate tests (shake test and Ultra Turrax), and slow foaming method (foam rise method) to assess the foamability at various bulk concentrations. The foamability data obtained from different foaming tests, utilizing various surfactant and polymeric concentrations, and differing foaming times, were shown to follow a universal master curve when plotted as relative foamability vs. scaled concentration. A new simple theoretical equation was derived to describe this universal curve, allowing for foamability prediction. The threshold surfactant concentration required to achieve 50% of the maximal foam volume under given conditions (used for scaling the bulk concentration) was found to decrease with foaming time and increase from slow foaming methods to fast foaming methods. When the experimental data are plotted against surface coverage, the results for PVA solutions exhibit intermediate behavior between nonionic surfactants, where a threshold surface coverage of 95% is required to achieve 50% of maximal foamability and anionic surfactants, where 30% surface coverage is sufficient to reach 50% of maximal foamability due to the action of electrostatic repulsion. This intermediate behavior observed in PVA solutions is attributed to the presence of a long-range steric repulsion arising from the adsorption of PVA

* Correspondence to: Department of Chemical and Pharmaceutical Engineering, Faculty of Chemistry and Pharmacy, Sofia University, 1 James Bourchier Ave., 1164 Sofia, Bulgaria.
E-mail address: SC@LCPE.UNI-SOFIA.BG (S. Tcholakova).

https://doi.org/10.1016/j.colsurfa.2023.132828
Received 24 September 2023; Received in revised form 16 November 2023; Accepted 18 November 2023
Available online 20 November 2023

molecules onto the bubble surfaces. This work advances the foam field by showing that the approach developed in Petkova et al. 2020 can be used for polymeric molecules and by deriving a new equation for foamability which is expected to be applicable for wide range of systems.

1. Introduction

The foams are widely studied in the literature due to their importance in different industries [1–5] and can be formed by various methods able to ensure the required energy for creation of new bubble surface area such as bubbling [6–11], rotating cylinders [12–14], shaking test [9,15–20] or pouring the liquid [21–23]. In all methods the foaming process consists of several consecutive stages: (1) gas entrapment or injection; (2) coalescence of trapped gas with ambient atmosphere; (3) fragmentation of large gas bubbles into smaller bubbles; (4) coalescence of smaller bubbles, forming larger bubbles with reduced surface area. First two processes determine the foam volume, whereas the last two processes define the mean bubble size in the formed foam [24]. The air entrapment and the coalescence of entrapped air depend on the rates of surfactant adsorption and bubble formation [15,16]. In our previous studies [15,16] we found that the foam volume increases almost linearly when dynamic surface coverage increases above 30% for ionic surfactants (anionic and cationic), whereas a step wise increase in foam volume is determined at surface coverage $>$ 95% for nonionic surfactants. This difference is explained by the mechanism of films stabilization: short range steric repulsion for non-ionic surfactants and long-range electrostatic repulsion for ionic surfactants [15].

The characteristic time for bubble formation depends significantly on the applied method for foam generation and, as a consequence, the dynamic surface coverage for given surfactant varies in the different methods. Long chain nonionic surfactants (such as Brij 58 and Tween 60) are unable to create voluminous foams in the fast foaming methods, such as Bartsch test, in which the characteristic time for bubble generation is very short and the bubble formation is accompanied with significant surface expansion, while the same surfactants form voluminous foam with small bubbles when Kenwood mixer is used, in which the characteristic time is much longer and the surface expansion is intermediate [16].

It is not clear in advance whether the developed approach for low-molecular mass surfactants can be directly applied to foams formed from polymeric solutions. Most of the polymers are slow adsorbing substances, due to their higher molecular mass as compared to low-molecular mass surfactants. The polymers can also interact strongly after their adsorption on the bubble surface and provide adsorption layers with various surface properties, such as surface elasticity, surface viscosity and surface yield stress – it is not known in advance how these properties will affect the air entrapment, bubble-bubble coalescence and bubble breakage in the course of foam generation [25–32].

Polyvinyl alcohols (PVA) are water-soluble polymers with wide range of applications because of their non-toxicity, biocompatibility and biodegradability [33]. These polymers are reaction products of polyvinyl acetate hydrolysis and can be synthesized with different molecular masses and different degrees of hydrolysis (DH). The foam behavior of four PVA polymers is studied in Ref. [34]. It was shown that the PVA solutions with a moderate degree of hydrolysis can be used to prepare foams with air volume fraction between 60% and 80% by high-speed mechanical agitation.

The aim of the current study is to compare the foamability of PVA solutions with those of low-molecular mass surfactants in several foaming methods and to analyze whether the proposed approach for low molecular mass surfactants in Refs. [15,16] could be applied to describe the behavior of foams formed from PVA solutions. The surface and foam properties and the role of hydrodynamic conditions are also analyzed. Several foaming methods are used which differ significantly not only in the timescale for bubble formation but also in the hydrodynamic conditions during foaming.

2. Materials and methods

2.1. Materials

Two groups of molecules were used as foam stabilizers: low molecular-mass surfactants and polymers from polyvinyl alcohols (PVA) series. The first group includes the anionic sodium lauryl ether sulfate (SLES) which is widely used in detergent formulations for home and personal care and the nonionic polyoxyethylene-23 lauryl ether (Brij 35). The second group consists of PVA with different molecular masses and degrees of hydrolysis, see Table 1.

To characterize the foamability and surface properties of the low molecular mass surfactants (SLES, Brij 35), initially a stock solution with 10 g/L concentration was prepared on a magnetic stirrer for 15 min at 40 °C and then it was diluted down to the working concentration with deionized water. For the polymers with 88% degree of hydrolysis (PVA 4–88, PVA 8–88, PVA 18–88, PVA 40–88) a 50 g/L stock solution was prepared by stirring for 4 h at 65 °C. Afterwards the samples were diluted down to the working concentration and stirred on a magnetic stirrer for 15 min at room temperature. The initial polymer solutions with 98% DH (PVA 4–98, PVA 10–98) were prepared at 10 g/L concentration and stirred on a magnetic stirrer for 2 h at 95 °C.

2.2. Methods

2.2.1. Dynamic and equilibrium surface tensions

The equilibrium surface tension (SFT), σ_{AW}, was measured by Wilhelmy plate method on a tensiometer K100 (Krüss GmbH, Germany) up to 1800 s. The equilibrium value for each measurement was determined from the intercept of the linear fit of the experimental data plotted as $\sigma \sim \frac{1}{\sqrt{t}}$ assuming diffusion limited adsorption [35]. The dynamic surface tension was measured by maximum bubble pressure method (MBPM) on BP100 (Krüss GmbH, Germany). Hydrophobized glass capillary with a hydrophilic tip was used to ensure bubble attachment to the capillary [36]. The air bubbles were blown through the capillary dipped inside the studied solution. The surface tension was measured as a function of a surface age, which is defined as the time from the start of the bubble formation to the occurrence of the pressure maximum. The dependence of surface tension on surface age was measured by varying the speed at which bubbles were produced.

Table 1
Characteristics of the studied foam stabilizers.

Type	Name	MW, g/mol	mM in 5 g/L	5 g/L solution viscosity, mPa.s	Supplier
Anionic	SLES	332	15.06	0.85	Stepan
Nonionic	Brij 35	1225	4.08	0.88	Sigma-Aldrich
	PVA 4–88	31,000	0.16	0.96	
	PVA 8–88	67,000	0.07	1.02	
	PVA 18–88	130,000	0.04	1.18	
	PVA 40–88	205,000	0.02	1.38	
	PVA 4–98	27,000	0.19	0.92	
	PVA 10–98	61,000	0.08	1.09	

The experiments for measuring equilibrium and dynamic surface tensions were performed at $T = 25 \pm 1$ °C by using thermostated cells.

2.2.2. Thin foam films in capillary cell

Foam films were formed and observed in the capillary cell of Scheludko-Exerowa [37]. The films were formed in a capillary with radius $R = 1.5$ mm by sucking out the solution through side orifice and were observed in reflected light with optical microscope Axioplan (Zeiss, Germany), equipped with a long-distance objective Zeiss Epiplan 20 × /0.40, CCD camera (Sony SSC-C370P) and 5.1 M Video Biological Microscope Digital Camera 55FPS LCMOS. The typical radius of the foam films formed in this capillary was $R_F \approx 0.15$ mm. By analysing the intensity of the reflected light, the foam film thickness was determined [37]. The film thinning pattern and the stability of the foam films were studied first with closed cell in which the capillary pressure was around 50 Pa then the cell was opened to the atmosphere which leads to capillary pressure increase up to 50,000 Pa due to induced water evaporation [38]. The experiments were performed at ambient conditions at 25 ± 2 °C.

2.2.3. Vertical foam films

The experimental setup for vertical films consists of a table, a vessel and a rectangular glass frame. First the frame is hanged on a hook, then the table is moved upwards until the solution covers the upper edge of the frame. The films are formed by moving the table downwards. Special precautions are taken to prevent evaporation from the film surfaces during the experiment. The films are observed by means of a video camera (5.1 M Video Biological Microscope Digital Camera 55FPS LCMOS) through the optical glass wall of the experimental cell. During the liquid drainage a particular pattern of the film thinning, is observed due to the combined action of the capillary suction of the bottom meniscus and gravity until a spot of thin black film is formed at the top of the frame [38]. Depending on the composition of the aqueous solution, a film rupture can be observed during the thinning process or after reaching its final equilibrium state. Under appropriate conditions (e.g. at high surfactant concentrations, mixture of surfactants, etc.) the formed films could remain stable for a very long period of time.

2.2.4. Foam tests for foam formation and stability

In the present work four different foaming methods were used for comparing the foam properties of surfactant and PVA solutions.

2.2.4.1. Bartsch test. In the current study we used new Bartsch test, in which 6 cylinders simultaneously are shaken, see Fig. S1 in supporting information. The principle of the method is the same as that explained in our previous papers [15,16], in which only 1 cylinder is shaken. In the new Bartsch test the time scale for bubble expansion is longer as compared to the previous test, because of the heavier construction - the air entrapment occurs under lower hitting force of the cylinder. The time scale is found to be of ≈ 1.8 s in the presence of bubble expansion, which is ≈ 5 times longer as compared to the previous test. The maximal amount of foam formed in this test is also lower as compared to the previous one (95 mL vs 120 mL). To be sure that the approach that has been developed in Ref. [16] can be applied for the new Bartsch test, we performed experiments with SDS, Brij 35, Brij 58 and Tween 20 with the new experimental set-up and compare them with the results obtained with the previous set-up. The comparison is shown in Fig. S2. One sees that after accounting for the longer time scale for foam generation in the new test and for the smaller amount of air that can be incorporated in the foams, the results from the previous and the current test follow the same trends for the studied surfactants, see Fig. S2B. Note that according to the model developed in Ref. [16], the milder conditions in the current test lead to higher amount of entrapped air in solutions of slow adsorbing surfactants (such as Brij 58) and to smaller foams in solutions of fast adsorbing surfactant due to the lower hitting force (such as SDS). Indeed, such behavior is observed in the current test, see Fig. S2A.

In the current study all experiments are performed with 10 mL surfactant solution in a 120 mL glass cylinder. The amount of entrapped air was determined as a function of the shaking cycles in the range between 10 and 1000 cycles. The volume of entrapped air was calculated by subtracting the volume of the solution (10 mL) from the total measured volume of the foam (solution + bubbles). The total measured volume was accounted first on every 10 cycles up to 200 cycles, then on every 50 cycles up to 1000 cycles.

2.2.4.2. Vertical shake test. A vertical shake machine Bioblock Scientific was also used to evaluate the foaming ability of the surfactant and PVA solutions, see Fig. S1B. This automatic device performed vertical shakes of 50 mL plastic tubes filled with 20 mL surfactant solution at 700 rpm for up to 1000 s and the foam volume was accounted first on every 10 s up to 200 s and then on every 50 s up to 1000 s [9]. The amplitude in the shake test is much smaller compared to that in Bartsch test and thus the deformation in the bubble area is smaller. Also, the free volume for bubble formation in the container is confined, leading to limited foamability.

2.2.4.3. Ultra Turrax. T25 digital Ultra Turrax was used to study the foamability of different surfactants. The principle of this method differs significantly from the other two methods described above. Here the air entrapment is due to the stirring by rotor instead of shaking. There is no big surface deformation and area expansion. The entrapment of small bubbles leads to much smaller mean bubble size in the formed foams, as compared to the other two methods. The studied solutions (20 mL) were placed in a 100 mL glass cylinder cut to 80 mL. When the tool is immersed in the liquid, the level goes up to 50 mL, so that the maximal foam volume is 30 mL. Then the solution is stirred at 20,000 rpm for 120 s. The foam volume was accounted after 30, 60 and 120 s

2.2.4.4. Foam rise. Dynamic Foam Analyzer DFA100 (Krüss GmbH, Germany) was used as foam rise (or bubbling method) and its principle is described elsewhere [16]. The main difference with the other used foaming methods consists in the much milder conditions during the foam generation - slower bubble formation without significant surface deformation. The bubbles are blown through a membrane and monodisperse foam is formed. After the bubble formation, there is an additional period for surfactant adsorption due to the floating of the bubbles through the entire solution. The foaming procedure was the same as described in [16]: 50 mL surfactant solution was poured into the cylinder and the gas with flow rate of 0.3 L/min was supplied through a frit of porosity G2 (40–100 μm pore size) under pressure. The foaming curve starts with an initial jump in the frame of several hundred milliseconds due to the gas supply, but the foamability is accounted after 1 s, where the foam level is well defined as described in ref [16]. The bubbling continued for 10 s and afterwards the foam decay was recorded for 600 s after stopping the gas supply.

All foaming experiments were performed at 25 ± 0.5 °C.

3. Results and discussion

3.1. Surface tension isotherms

The surface tension as a function of time was measured for 30 min by Wilhelmy plate method. The results for the surface tension were plotted as a function of $1/t^{1/2}$ for $t > 800$ s and from the intercept the equilibrium surface tension, σ_{EQ}, was determined, see Fig. S3. The surface tension isotherms for PVA and surfactant solutions are shown in Fig. 1.

The surface tension isotherms for PVA solutions differ significantly from those of low molecular mass surfactants, where a clearly defined plateau region is reached above the critical micellar concentration. In contrast, for PVA solutions, the surface tension diminishes with

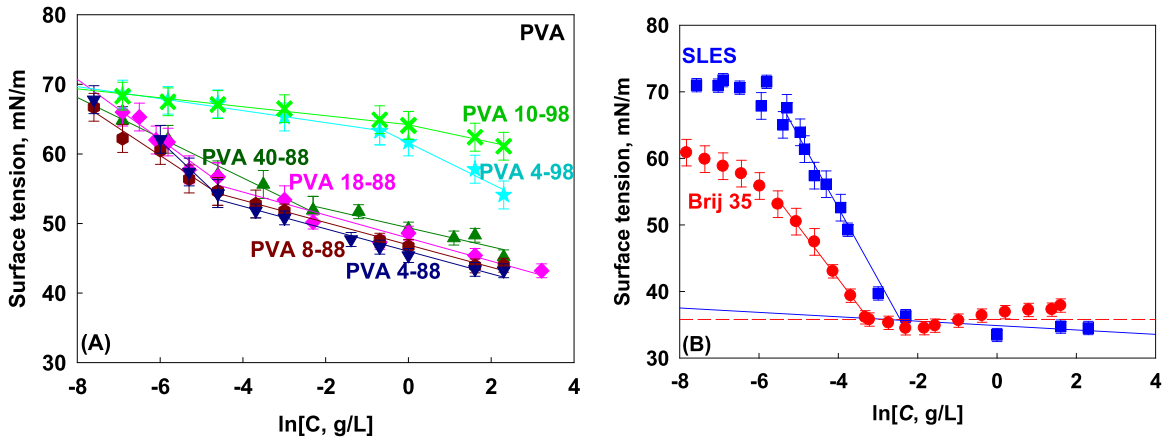

Fig. 1. Surface tension isotherms for the systems studied: (A) PVA solutions with different degrees of hydrolysis and different molecular masses: PVA4–98 (cyan stars), PVA10–98 (green crosses), PVA40–88 (dark green triangles), PVA18–88 (pink diamonds); PVA8–88 (dark red hexagons), PVA4–88 (dark blue inverted triangles); (B) surfactant solutions: Brij 35 (red circles) and SLES (blue squares).

increasing PVA concentration in the entire concentration range. The lowest surface tension achieved at the highest PVA concentration, C_P, is significantly higher for PVA with a 98% degree of hydrolysis (DH) in comparison to PVA with 88% DH. The surface tension of PVA with 98% DH (PVA 10–98 and PVA4–98) remains above 65 mN/m up to 0.1 g/L and starts to decrease afterwards. However, for PVA with 88% DH, the decrease in σ_{EQ} against lnC_P is more pronounced at low concentrations, while PVA with 98% DH exhibits a notably smaller initial slope in comparison to the steeper slope observed at higher polymer concentrations. The lack of a plateau in σ_{EQ} versus lnC_P for polymeric solutions is well-documented in the literature [39–43]. The presence of two distinct regions with different slopes in the surface tension isotherms of polymers has been frequently observed experimentally and attributed to different factors. These include the depletion of polymer molecules at lower concentrations [44], preferential adsorption of rapidly adsorbing molecules with lower molecular weight at lower polymer concentrations, and the preferable adsorption of higher molecular weights at higher polymer concentrations [40]. The point of transition, referred as the transition concentration (C_{TR}), shows the PVA concentration at which the slope of σ_{EQ} against lnC_P undergoes distinct alteration. It was shown that the structure and composition of adsorption layers formed at $C_P < C_{TR}$ and $C_P > C_{TR}$ differ significantly [40] for PVME (polyvinyl methyl ether). At low C_P the layer is thinner and contains mainly lower MW polymer molecules, whereas thicker adsorption layer is formed at high C_P.

The experimental data obtained in the current study shows that PVA with lower MW have lower C_{TR} which is in a good agreement with the predictions proposed in [40]. Therefore, we can conclude that at $C_P < C_{TR}$ the polymeric molecules with lower molecular weight are preferentially adsorbed on the solution surface, due to their faster adsorption. At $C > C_{TR}$ the adsorption of the higher molecular mass polymers takes place and the slope decreases for PVAs with 88% DH.

To characterize the formed adsorption layers in these two regions we determined the slopes of σ_{EQ} vs lnC_P for $C_P < C_{TR}$ and $C_P > C_{TR}$ and by applying the Gibbs adsorption isotherm we determined the apparent adsorption of polymer on the air-water interface:

$$\frac{d\sigma_{EQ}}{dlnC} = -k_B T\Gamma \quad (1)$$

Here σ_{EQ} is equilibrium surface tension, C is surfactant (C_S) or polymer (C_P) concentration at which this surface tension is measured, k_B is Boltzmann constant, T is temperature and Γ is apparent adsorption. The results for the transition concentration, C_{TR}, surface tension at transition concentration, σ_{TR}, the adsorption at low concentration range $C_P < C_{TR}$ and high concentration range $C > C_{TR}$ are shown in Table 2.

Table 2
Isotherm parameters: critical threshold concentration for polymer solutions, C_{TR}, or critical micellar concentration, CMC, for low molecular mass surfactants; surface tension at C_{TR}, σ_{TR}; adsorption, Γ, and area per molecule, α, as determined from Eq. (1) at $C < C_{TR}$ and at $C > C_{TR}$. All measurements are performed at 25 °C in deionized water.

System	σ_{TR}, mN/m	C_{TR}, mg/L	Γ_M, μmol/m^2		α, Å^2	
			$C < C_{TR}$	$C > C_{TR}$	$C < C_{TR}$	$C > C_{TR}$
PVA 4–88	53.2	12	2.3	0.7	52	240
PVA 8–88	54.3	10	1.6	0.6	82	240
PVA 18–88	55.2	12	1.7	0.7	72	235
PVA 40–88	53.3	57	1.2	0.5	120	287
PVA 4–98	63.3	560	0.3	1.2	434	117
PVA 10–98	64.4	940	0.3	0.5	592	290
SLES	35.7	88*	4.3	N.A.	38	N.A.
Brij 35	35.5	41*	3.2	N.A.	52	N.A.

N.A. – not applicable
* - threshold concentration for SLES and Brij is the critical micellar concentration CMC

One sees that $C_{TR} \approx 10$ mg/L for PVA4–88; PVA8–88 and PVA 18–88, approximately 5-times higher for PVA 40–88 with $C_{TR} \approx 50$ mg/L and more than 100-times higher for PVA with 98% DH where $C_{TR} > 500$ mg/L. The much higher values of C_{TR} for PVA with 98% shows that the polymeric molecules from these samples have much lower surface activity due to the very limited amount of polyvinyl acetate groups in these molecules.

The weight efficiency of Brij 35 and SLES is very high because these two surfactants are able to decrease the surface tension down to 35 mN/m at CMC ≈ 40 mg/L for Brij 35 and 88 mg/L for SLES. The transition surface tension varies between 53 and 55 mN/m for PVA with 88% DH and it is much higher (63 mN/m) for PVA with 98% DH. The apparent adsorption varies between 1.2 μmol/m^2 (PVA 40-88) and 2.3 μmol/m^2 (PVA 4-88) at $C_P < C_{TR}$ for PVA with 88% DH. These values are relatively high for polymeric solutions, showing again that the molecules with the lowest molecular mass are adsorbing initially on the solution surface. The values of Γ decrease at $C_P > C_{TR}$ and become between 0.5 and 0.7 μmol/m^2 for PVA with 88% DH. These values are in a good agreement with the results reported by De Feijter & Benjamins [41] for PVA solutions with similar MW and DH (88% DH and MW between 42 and 200 kDa) for which Γ between 0.5 and 0.6 μmol/m^2 were determined from the surface tension isotherms.

Therefore, depending on the foaming method we could expect that the composition of the adsorption layers will be different – for fast adsorbing methods we could expect that the smaller molecules will adsorb on the bubble surface because of their faster diffusion, whereas in the slow foaming methods larger molecules will prevail in the adsorption layer.

The experimental data obtained with low molecular mass surfactants SLES and Brij 35 are also shown in Table 2. Note that values obtained for Brij 35 differ significantly from the data shown in the literature [15]. In this reference it is shown that Brij 35 area per molecule is around 80–90 Å^2, while the measured area in the current study is ≈ 50 Å^2. The surface tension is also much lower, 42 mN/m vs. 36 mN/m. A possible explanation is the difference in the products composition, despite the fact that both samples are purchased from Sigma -Aldrich as Brij 35. A closer look reveals that the one used in our work is with product number 1254, denoted as suitable for Stein-Moore chromatography, which implies a single component sample, while the one used in the work of Petkova et al. [15] was with product number 16005 denoted as main component: tricosaethylene glycol dodecyl ether, which probably means that it contains different components. This difference could be the reason for the much smaller area per molecule, higher adsorption and lower surface tension in the current study compared to the previously reported. However, as shown in Fig. S2 when we re-plotted the relative foamability as a function of surface coverage for the new and the old batch of Brij 35 in the new and the old Bartsch test, they fall on the same universal master curve, which means that the impurities in the new batch of Brij 35 do not affect the general trends, probably because they have significant impact not only on the equilibrium adsorption layer, but also on the dynamic surface layer. The data determined for SLES are in good agreement with the results reported in the literature for the CMC, the surface tension at CMC [45] and adsorption at CMC [46].

To determine the surface coverage during foaming we have to know what is the relation between the measured surface tension and surfactant adsorption. In our previous studies [15,16] we used the Volmer adsorption isotherm to define this relation:

$$\frac{\pi}{k_B T} = \frac{\Gamma}{1 - \alpha\Gamma} \tag{2}$$

Here π is the surface pressure defined as a difference between the surface tension of pure water, σ_0 and the measured surface tension, σ; α is the limiting area per molecule in the adsorption layer. For low molecular mass surfactants used in our previous study, the value of α was determined from the measured surface tension at CMC and the value of Γ at CMC by using Eq. (1). For the current study we used the same approach for Brij 35 and SLES, see Table 2.

For polymeric solutions, however, as discussed above there are two slopes in σ_{EQ} vs lnC_P below and above C_{TR}, which are related to different compositions of adsorption layers formed at low and high polymer concentrations. To account for this difference, we applied Eq. (2) in the two regions independently, assuming two different values of α and Γ_M in these two regions. At $C > C_{TR}$ the value of α is determined by applying Eq. (2) for $C = 10$ g/L, whereas for $C < C_{TR}$ the value of α is determined by applying Eq. (2) for $C = C_{TR}$. The obtained results for Γ_M and α in these two regions are presented in Table 2. These values are used afterwards to determine the surface coverage from the experimental data obtained with MBPM.

At $C < C_{TR}$, the limiting area per molecule, α, is much higher for polymers with higher DH, as compared to those with low DH, but at high polymer concentrations this difference disappears. At low concentrations, the increase of the molecular mass at given DH leads to increase in the area per molecule, whereas there is no such effect at $C > C_{TR}$.

3.2. Dynamic surface tension

The dynamic surface tension, DST, was measured by MBPM, as a function of the nominal surface age (t_{age}) which is defined for expanding bubble and one should transfer it to the universal surface age (t_u) which does not depend on the specific tensiometer and characterizes the kinetics of adsorption from the same surfactant solution on non-expanding solution surface [15,47]. For the used tensiometer, the relation between t_{age} and t_u is $t_u = t_{age}/37$ [47]. The obtained results are shown as a function of time in Fig. S4 in supporting information. The comparison of the dynamic surface tension at $C = 5$ g/L is shown in Fig. 2A, whereas DST at universal time of $t_u = 50$ ms corresponding to $t_{age} = 1.85$ s, which was found to be the characteristic time for foam generation in the new Bartsch test is shown, as a function of C, in Fig. 2B.

The dynamic surface tension is the lowest when low molecular mass surfactants Brij 35 and SLES are used. The DST for 5 g/L SLES and Brij 35 measured after 10 ms for these surfactants is ≈ 50 mN/m and it decreases to ≈ 37 mN/m after 10^5 ms. The highest DST is measured for PVA samples with 98% DH, it starts from 71 mN/m and decreases to ≈ 69 mN/m only after 10^5 ms. An intermediate behaviour is observed for PVA with 88% DH. For 5 g/L PVA with 88% DH, DST starts from 67 mN/m and reaches the value of ≈ 55 mN/m after 10^5 ms. The PVA samples with lower MW at fixed DH have lower DST, which supports the hypothesis that the smaller polymer molecules adsorb preferentially at shorter times. Note that even at this high polymer concentration of 5 g/L the lowest value of DST which is reached after 10^5 ms is around the threshold surface tension where the transition between the first and second concentration regions occurs. Therefore, for determination of the adsorption and surface coverage of the bubbles formed in the fast foaming methods, the parameters obtained from the surface tension isotherms at $C < C_{TR}$ are used.

The effect of polymer concentration on the properties of the adsorption layers was also studied and the results from these measurements are shown in Fig. 2B. DST decreases steeply with C for SLES solutions, whereas an almost linear decrease of DST vs ln$C$ is determined for Brij 35 and PVA solutions. The DST for Brij 35 is much lower at all studied concentrations as compared to PVA solutions. DST is the highest for PVA with 98% DH and intermediate for PVA with 88% DH for which the molecular mass has some impact on the measured DST – higher MW at fixed DH leads to higher DST, due to the slower adsorption of the bigger molecules. The observed lower surface activity of PVA with 98% DH, as compared to that for PVAs with 88% DH is in a good agreement with the results in literature [48,49]. Note that higher degree of hydrolysis corresponds to bigger fraction of alcohol groups at the expense of acetate groups. The increase in DH leads to increase in polymer solubility and to formation of hydrogen bonds, decrease in surface activity, and thus higher surface tension and lower adsorption is observed [48,49].

From the measured DST we calculated the instantaneous adsorption. This was done by using the calculated parameters for the equilibrium surface layers, given in Table 2 (for the first region $C < C_{TR}$), and assuming that the adsorption layers are similar to the layers formed at low polymer concentrations where the polymer molecules with lower molecular mass are preferentially adsorbed on the air-water interfaces. The estimated surface adsorption is shown in Fig. S5 and compared for 5 g/L solutions in Fig. 3 A. The calculated adsorption is very low ≈ 0.3 μmol/m^2 for PVA with 98%, but it is reached for less than $t_{age} < 10$ ms. On the other hand, the adsorption for PVA with 88% DH depends significantly on the PVA concentration and on the surface age. The adsorption starts from very low values for 0.1 g/L solutions and increases almost linearly with lnt_{age}. The increase of PVA concentration in the solution increases significantly the adsorption at $t_{age} = 10$ ms, while slightly increases the adsorption at $t_{age} = 10^5$ ms, which means that the effect of PVA concentration is more important for the foamability in the fast foaming methods as compared to the slow foaming methods.

The effect of bulk polymer concentration on the adsorption determined after $t_u = 50$ ms is shown in Fig. 3B. The adsorption is the highest for SLES, followed by Brij 35. The adsorption of PVA solutions with 88% DH varied between 0.8 and 2 μmol/m^2 – the adsorption increases with decreasing the average molecular mass of the polymer. Significantly

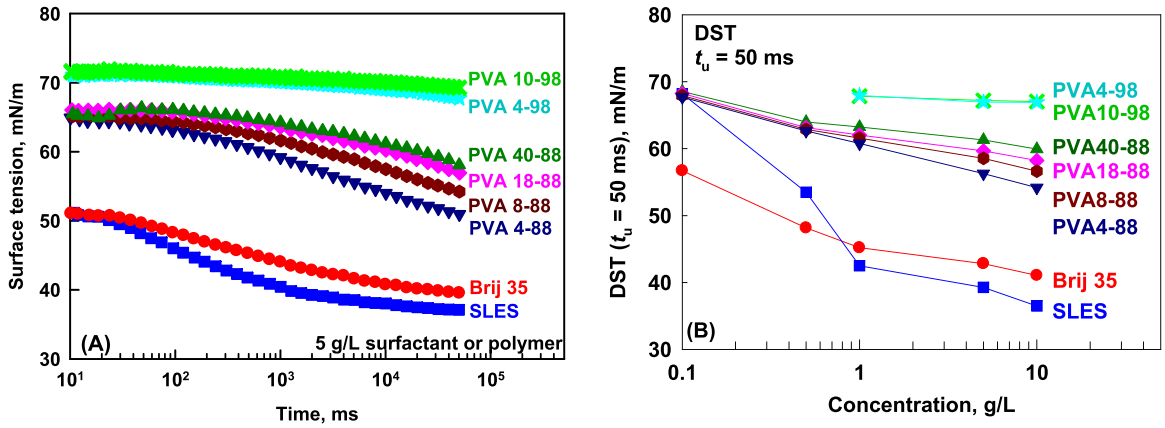

Fig. 2. (A) Dynamic surface tension as a function of time (nominal surface age) at $C = 5$ g/L and (B) DST measured after 50 ms universal surface age (corresponding to 1850 ms nominal surface age) as a function of surfactant or polymer concentration for PVA4–98 (cyan stars), PVA10–98 (green crosses), PVA40–88 (dark green triangles), PVA18–88 (pink diamonds); PVA8–88 (dark red hexagons); PVA4–88 (dark blue inverted triangles); Brij 35 (red circles) and SLES (blue squares).

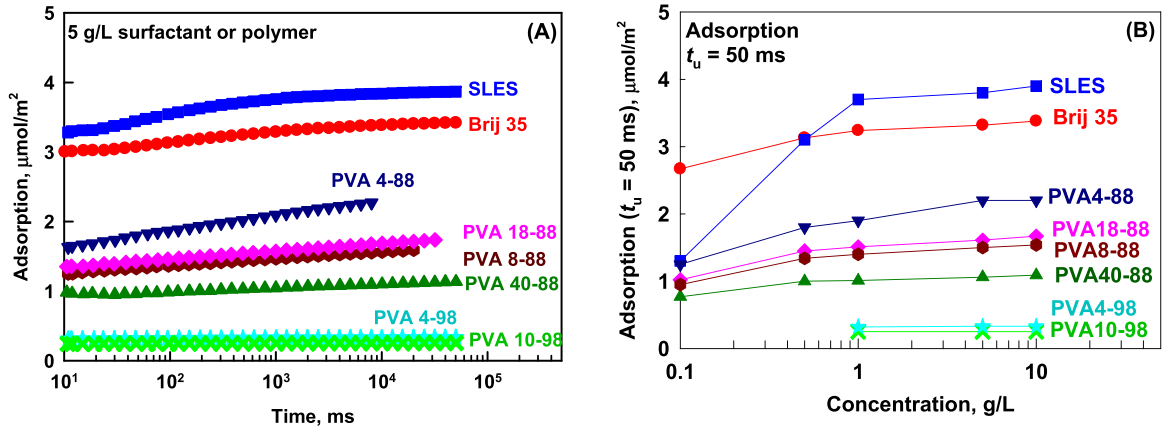

Fig. 3. (A) Instantaneous adsorption as a function of time (nominal surface age) at $C = 5$ g/L and (B) Instantaneous adsorption determined after 50 ms universal surface age (corresponding to 1850 ms nominal surface age) as a function of surfactant or polymer concentration for PVA4–98 (cyan stars), PVA10–98 (green crosses), PVA40–88 (dark green triangles), PVA18–88 (pink diamonds); PVA8–88 (dark red hexagons); PVA4–88 (dark blue inverted triangles); Brij 35 (red circles) and SLES (blue squares).

lower adsorption is determined for PVA solutions with 98% DH.

From these series of experiments, we can conclude that PVA with 88% DH has much higher surface activity as compared to PVA with 98% DH which leads to much lower equilibrium and dynamic surface tension measured and much higher instantaneous adsorption for PVA with 88% DH. There are two slopes in σ_{EQ} vs $\ln C_P$ showing the different composition of the adsorption layers formed at low and high PVA concentrations: at low $C_P < C_{TR}$ the preferential adsorption of low molecular mass polymeric molecules occurs, whereas at $C_P > C_{TR}$ the higher molecular weight molecules adsorb and further decrease the surface tension. The transition concentration is lower for PVA with 88% DH as compared to PVA with 98% DH.

3.3. Foam films in capillary cell

The behavior of horizontal foam films was studied in Sheludko cell. The illustrative pictures from these experiments are shown in Fig. 4 and Fig. S6 in Supplementary information. The rate of film thinning is much faster for films formed from SLES and Brij 35 solutions and the final thickness that is reached in closed cell at capillary pressure of $P_C \approx 50$ Pa is much lower, $h \approx 30$ nm as compared to the thickness of the films formed from all PVA solutions. At this pressure thicker films are formed from PVA 40–88, $h > 100$ nm, which has the highest average molecular mass. This large film thickness evidences that the adsorbed polymers ensure long range steric repulsion. The decrease of average molecular

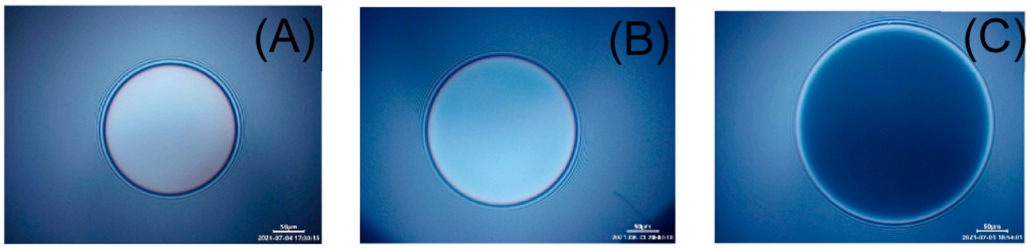

Fig. 4. Illustrative images of foam films formed in capillary cell after opening it to the atmosphere for films formed from 5 g/L solutions of (A) PVA40–88; (B) PVA18–88 and (C) PVA 8–88.

mass leads to formation of films with smaller equilibrium film thickness which means that the steric repulsion is induced from smaller polymeric molecules.

All formed films remain stable in closed cell. After cell opening to the atmosphere, the compression pressure increases and the film thickness decreases for all polymers and surfactants studied. The films formed from PVA solutions with 98% DH are unstable at that stage, which means that the lower adsorption on the surface is insufficient to induce steric repulsion which could overcome the compressing pressure of 10^5 Pa. Fraction of the films formed from PVA 4–88 which has the lowest average molecular mass, was also unstable despite the higher adsorption determined from surface tension measurements, which shows that the lower molecular mass polymeric molecules can adsorb faster on the bubble surface but cannot create sufficient steric repulsion to prevent the film rupture after compression to 10^5 Pa. All films stabilized by PVA8–88; PVA18–88 and PVA 40–88 and those by SLES and Brij 35 remain stable even after opening the cell, which means that the repulsive barrier in the disjoining pressure isotherm is higher than 10^5 Pa. However, the equilibrium film thickness at 10^5 Pa differs significantly for various surfactants – it is the smallest for Brij 35 implying that a short-range steric repulsion is responsible for stabilization of these films, intermediate for SLES show that the electrostatic repulsions are operative for those films and much thicker for PVA40–88 meaning that a long-range steric repulsion is responsible for stabilization of PVA with 88% DH and relatively high molecular mass.

3.4. Vertical foam films

The behavior of films formed in capillary cell is relevant for determining the forces that stabilize the bubbles in the slow foaming methods, because the rate of film expansion in the capillary cell is relatively low and the time for adsorption of surfactant and polymer species is long enough to ensure the equilibrium adsorption at a given concentration. In the fast foaming methods, the rate of bubble expansion is much higher and the foam films are usually bigger, due to the entrapment of large bubbles. To compare the ability of low molecular mass surfactants and PVA solutions to stabilize the foam films during the surface expansion we performed experiments by using the procedure described in Section 2.2.3. The illustrative images of the film thinning behavior are shown in Fig. S7 in supporting information.

For surfactant systems the highest dynamic film stability is observed with the anionic surfactant SLES for which the films succeed to drain and to reach smaller thickness before rupture. On the other hand, for Brij 35 the film rupture occurs at much larger thickness. The least stable films are those stabilized by PVA 18–88 which rupture almost immediately after their formation, which is in a good agreement with the slower rate of PVA adsorption as compared to Brij 35 (as determined by DST measurements, see Fig. 3 A). The probability for film rupture is shown in Fig. 5. One sees that 100% of the formed films from PVA 18–88 solutions rupture for less than 1 s after their formation, whereas all studied films from SLES remain stable for at least 80 s after their formation.

From these series of experiments, we can conclude that the instantaneous adsorption of PVA is lower as compared to SLES and Brij 58 and, as a consequence, the stability of the vertical films is also lower. The horizontal films formed from PVA solutions are stable at low compressing pressures and the equilibrium thickness increases with the molecular weight at a given DH. The small horizontal films rupture when higher compressing pressure is applied for PVA with 98% DH. The higher molecular weight of the PVA leads to formation of thicker horizontal films, due to the action of long-ranged steric repulsion between the film surfaces.

3.5. Foam properties

The foam properties were evaluated by using 4 different tests which differ significantly in the rate of bubble expansion during the air entrapment and bubble formation. Bartsch test (BT) is a fast foaming method, foam rise method (FRM) is a slow foaming method with limited expansion of the surface area upon bubble formation, whereas the shake test and UT homogenization are intermediate between the Bartsch test and FRM.

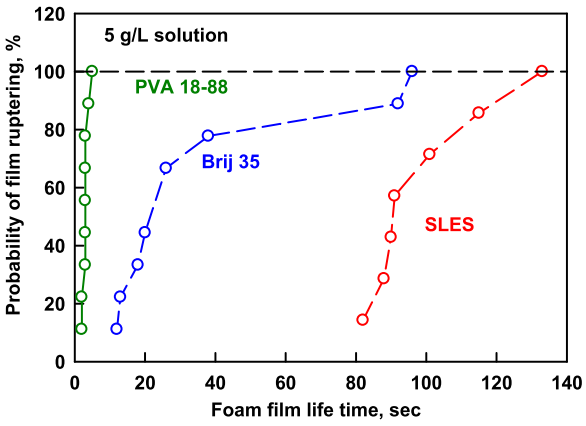

Fig. 5. Probability for rupture of vertical films formed from 5 g/L SLES (red symbols), 5 g/L Brij 35 (blue symbols) and 5 g/L PVA18–88 (green symbols) solutions after a certain time.

3.5.1. Foamability in Bartsch test

The experimental results for the volume of entrapped air, V_A, as a function of the number of shaking cycles, n, for the studied PVA and surfactant solutions are shown in Fig. 6 and Fig. S8. Foamability of PVA 4–98 is very low at all studied C_P and n. Some increase in V_A with n is observed for PVA 10–98 with $C_P \geq 5$ g/L, whereas V_A remains very low ($\approx$ 10 mL) even after 1000 cycles for 1 g/L PVA 10–98 solutions. For PVA with 88% DH, V_A remains very low ($\approx$ 10 mL) even after 1000 cycles only for $C_P = 0.1$ g/L, whereas significant increase in V_A with n is determined at higher concentrations (the exception is 0.5 g/L PVA 4–88 where V_A remains $\approx$ 10 mL). The initial fast increase of V_A in the first 100 cycles is usually accompanied with much slower further increase in V_A in the last 900 cycles for most of these solutions. For some of them V_A remains almost constant after 100 cycles. The behavior of Brij 35 stabilized foams is very similar to that of PVA solutions with 88% DH, whereas the foamability of SLES solutions is much higher and the rate of foam generation is very fast for $C_S \geq 0.5$ g/L. To compare the initial, intermediate and final foamability of the studied solutions we determined the values of V_A after 10, 100 and 1000 cycles and the results are shown in Fig. 6B and S9 in supporting information.

After 10 shaking cycles, the foamability of PVA and Brij 35 solutions at $C \leq 1$ g/L is very low ($V_A < 20$ mL), whereas it is much higher when 1 g/L SLES is used ($V_A = 65$ mL). The further increase of PVA concentration in the solution to 10 g/L leads to different values of V_A depending on the type of PVA used. The volume of entrapped air at 10 g/L after 10 shaking cycles is the lowest for PVA 4–98 and the highest for PVA 40–88, which shows that the higher molecular mass and the lower DH facilitate the air entrapment at short times for polymeric solutions.

At 100 and 1000 shaking cycles, V_A for PVA 4–98 remains constant as a function of C and does not increase with the number of shaking cycles. The increase of molecular mass in PVA10–98 at the same DH increases the foamability, especially at $C > 1$ g/L. Almost linear increase of V_A vs lg$C$ is observed for PVA (except for PVA 4–98) and Brij 35. Much steeper increase in V_A is observed for SLES solutions - the maximal V_A is reached at $C = 1$ g/L after 1000 cycles.

From this series of experiments, we can conclude that SLES is the most efficient surfactant for the formation of voluminous foam in the initial stage of the foaming process in the fast foaming method such as Bartsch test. Brij 35 and PVA 40–88 are unable to entrap sufficient amount of air in the initial stage of the foaming process, but at higher

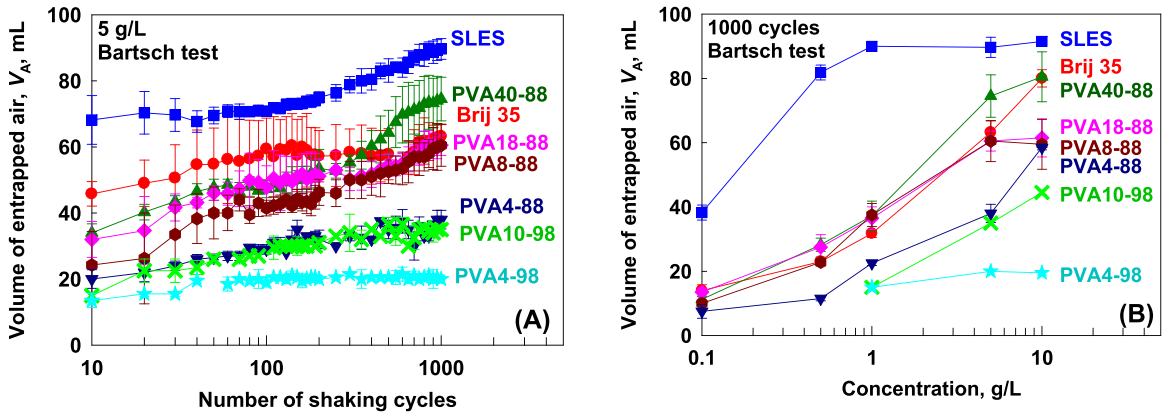

Fig. 6. Volume of entrapped air as a function of (A) number of shaking cycles in Bartsch test for solutions containing 5 g/L surfactant or polymer and (B) concentration for foams formed in Bartsch test after 1000 cycles for various surfactants and PVA samples as indicated in the figures.

concentrations and longer foaming times these solutions can incorporate more than 85% of the maximal volume of air that can be incorporated under these conditions. PVA 4–98 is very inefficient as foam stabilizer in this method, because the entrapped air remains below 20 mL even at 10 g/L. The higher molecular mass and lower degree of hydrolysis facilitate the air entrapment in PVA solutions in Bartsch test.

3.5.2. *Foamability in shake test*

In both the Bartsch test and the shake test the foam is generated by vertical periodical shakes (of the cylinder in Bartsch test and centrifugal tube in shake test). However, in Bartsch test the cylinder is moved at more than 90 degrees and, during the foam generation, there is a splashing of the liquid over the liquid surface when the cylinder hits the stopper in the equipment. In contrast in the shake test the angle of rotation is around 6° only, as a consequence, the rate of expansion of the newly created surface is smaller and the time during which the surfactants can adsorb on the bubble surface is longer. The other difference is that, in the Shake test the maximum entrapped air is constrained by the tube capacity (50 mL plastic tube) to 30 mL, while in Bartsch test the maximum V_A is 110 mL. Note, however, that the later volume cannot be reached in the current version of the experimental set-up due to its heavier construction - the maximum volume of entrapped air is 95 mL, as explained in section 4.5.1 above. The experimental data obtained in the shake test are shown in Fig. S10 in Supporting information.

After 10 shaking cycles, the foamability of SLES with $C \geq 0.5$ g/L reaches the maximum V_A for this equipment of 30 mL. The dependence of V_A vs C is very similar for Brij 35 and PVA18–88 as can be seen from the data presented in Fig. S10. The foamability of PVA 10–98 is lower as compared to that of PVA 18–88, while being higher as compared to PVA 4–98. Therefore, similar rating of the foamability of the studied solutions is observed – faster foam generation with SLES solutions, intermediate with PVA at 88% DH and Brij 35, and the lowest with PVA at 98% DH. The higher molecular mass leads also to better stabilization of the foams formed.

The concentration dependences after 50, 100 and 1000 cycles are somewhat different as compared to that determined after 10 cycles. The main difference arises from the fact that the foamability of Brij 35 and PVA 18–88 increases with increasing the number of shaking cycles, becoming close to that observed with SLES solution, whereas the foamability of PVA with 98% DH remains lower even after 1000 cycles. Some increase in the foamability of PVA with 98% DH is also observed with the increase of the shaking cycles, but this foamability remains lower as compared to that of the intermediate group (Brij 35 and PVA18–88). The difference between PVA4–98 and PVA10–98 which is well pronounced up to 100 cycles also disappears after 1000 cycles. Therefore, the difference between the studied solutions diminishes with the number of shaking cycles.

3.5.3. *Foamability in Ultra Turrax*

The foams prepared in Ultra Turrax contain much smaller bubbles as compared to the previous two methods (shake test and Bartsch test). The foam formation take place inside the solution due to the element rotation and is accompanied with much smaller surface deformation when compared with to the shaking methods. The mean bubble size is determined by the gap between the rotor and stator and after their formation the bubbles float through the solution up to the surface, thus ensuring additional period for adsorption of surfactant or polymer on the surface of the created bubbles. The experimental results from this method are shown in Fig. S11.

The foamability of SLES and Brij 35 after 30 and 60 s of solution stirring are very similar at $C \geq 0.05$ g/L, whereas at $C = 0.01$ g/L again the best foamability is observed with SLES solution. After 30 s of stirring, there is no significant difference in the foamability of the PVA solutions with 88% and 98% DH, whereas after 60 s of stirring PVA 18–88 shows better ability to stabilize the formed bubbles as compared to PVA 4–98 and PVA 10–98, but it is still lower when compared to Brij 35. At 10 g/L concentration the maximal available foam volume (30 mL) is reached for all systems, which means that even PVA with 98% DH can stabilize the small bubbles formed in UT.

3.5.4. *Foamability in bubbling method (foam rise method)*

The conditions for foam generation in the bubbling method are the mildest. It creates bubbles via blowing air into the solution through a membrane with defined pore size. This method ensures the formation of nearly monodisperse bubbles, which during floating through the solution can be covered by adsorbed surfactant molecules. The characteristic time for this process is ≈ 50 s during Wilhelmy plate measurements as shown in ref [16].

The experimental results for the foam volume as a function of time during the gas injection up to 10 s and after stopping the gas injection (after 10 s) is shown in Fig. S12 and Fig. 7. The amount of stable gas bubbles increases with time at concentrations above 0.01 g/L. At lower concentrations, the surfactants are unable to stabilize the injected bubbles even in this slow-foaming method. Best bubble stabilization is observed with SLES solutions, followed by Brij 35 and the lowest stability is determined for PVA 18–88, see Fig. 7B.

3.6. *Comparison of the results, obtained in different methods*

To compare the foaming ability of the studied surfactant and PVA solutions in the various methods, we used the approach developed in Ref. [16] and determined the relative foamability defined as the foam volume divided by the volume of the foam generated from 10 g/L SLES solution in a given test after the longest time used in this test. For Bartsch test V_{MAX} is 95 mL; for the shake test and UT it is 30 mL and for the FRM

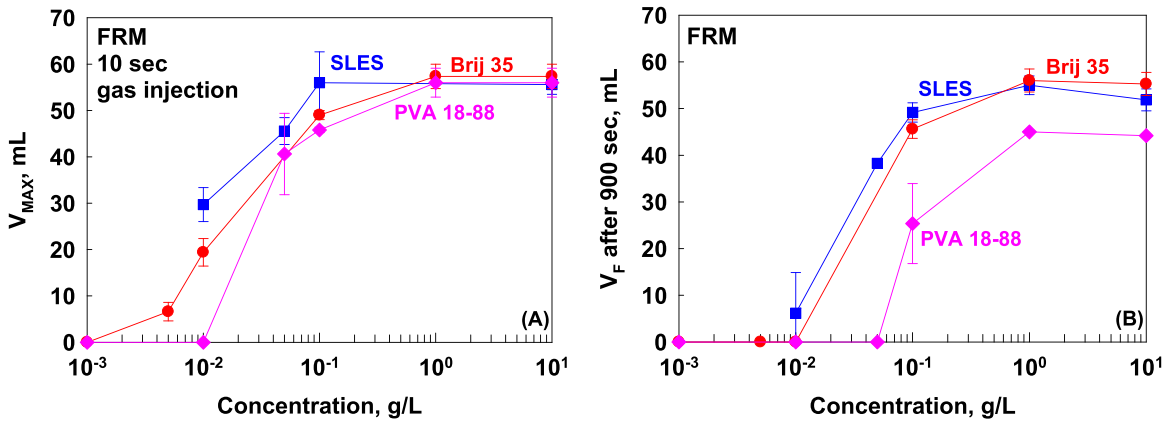

Fig. 7. (A) Maximum foam volume reached after 10 s of gas injection and (B) Final foam volume at 900 s after stopping the gas injection, as a function of surfactant concentration in Foam Rise Method.

it is 55 mL. The relative foamability as a function of surfactant or polymer concentration for PVA 18–88; SLES and Brij 35 in the 4 different tests is shown in Fig. 8 (after 1000 cycles) and Fig. S13 (after 10 cycles). One sees that the relative foamability is lowest in Bartsch test, intermediate in shake test and UT and the highest in FRM for all studied surfactants and all studied foaming times at a given concentration. In all tests the curves have similar shape – very low foamability below a certain concentration, an almost linear increase with the logarithm of bulk concentration at intermediate concentrations, and 100% foamability above a certain concentration. To compare the concentration dependence in the different tests we scale the actual concentration with the concentration required to reach 50% of the relative foamability in a given test, C_{50}.

The values of C_{50} for all studied tests are shown in Table 3 and Fig. S14. It can be seen that C_{50} decreases with increasing the number of shaking cycles in Bartsch and shake tests, and with stirring time in UT. The lowest values of C_{50} in all tests are determined for SLES. For this surfactant, the values of C_{50} varied between 0.01 g/L in FRM and 0.28 g/L in Bartsch test after 10 cycles. The effect of foaming time is relatively small for SLES solutions. The value of C_{50} decreases by approximately 2-times with the number of shaking cycles in Bartsch test from 10 to 1000.

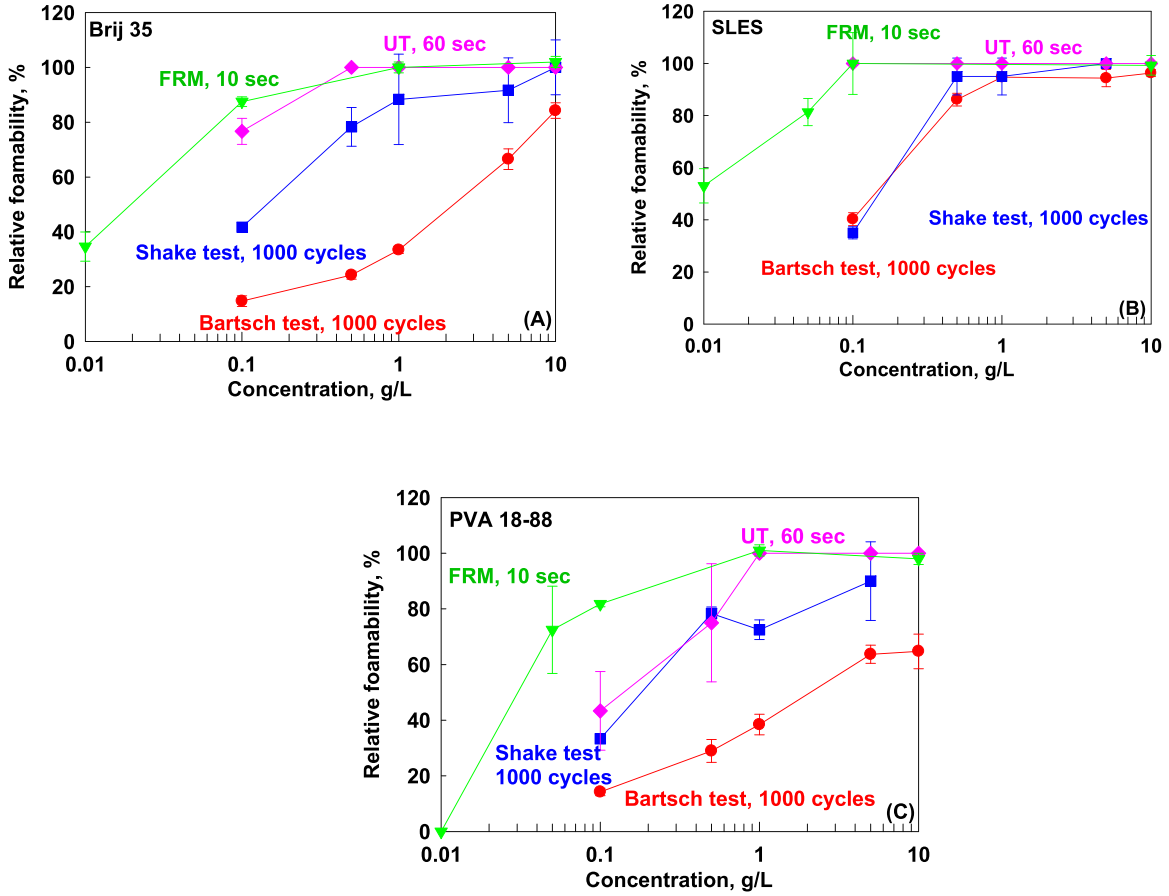

Fig. 8. Relative foamability as a function of concentration for (A) Brij 35; (B) SLES and (C) PVA18–88, as measured in different tests after 1000 shaking cycles at Bartsch and shake tests and after 60 s at UT. In all graphs the results for the maximum foam volume reached after 10 s of gas injection in FRM are shown.

Table 3
Concentration, C_{50}, at which the solutions form foams with 50% volume when compared to the maximum foam volume that can be reached in a given test under certain foaming conditions and estimated concentration, C_A, required to ensure formation of dense adsorption layer with $\Gamma = \Gamma_{TR}$.

	C_{50}, g/L								
	Bartsch test, cycles			Shake test, cycles			UT, s		FRM, s
Foaming time	10	100	1000	10	100	1000	30	60	10
SLES	0.37 ± 0.14	0.16	0.15	0.16	0.15	0.1	0.03	0.01	0.01
Brij 35	5.6	2.9	2.3	1.26	0.16	0.15	0.09	0.03	0.02
PVA 18–88	20.0	5.0	2.0	1.20	0.29	0.18	0.57	0.15	0.03
	C_A, g/L								
	Bartsch test			Shake test			UT		FRM
SLES	0.04			0.01			0.01		0.02
Brij 35	0.11			0.02			0.04		0.04
PVA 18–88	6.30			1.00			1.99		2.43

In all tests, the values of C_{50} for PVA 18–88 are the highest. In Bartsch test after 10 cycles, the value of C_{50} for PVA is 20 g/L, which is by 70-times higher as compared to SLES concentration (0.28 g/L). The effect of the number of shaking cycles is more important for PVA 18–88 as compared to SLES. The increase of the number of shaking cycles from 10 to 1000 in Bartsch test decreases by 10 times C_{50} for PVA 18–88, whereas only 2-times decrease is observed for SLES. The values of C_{50} for Brij 35 are intermediate between those of SLES and PVA 18–88.

The values of C_{50} are used to determine the dependence of the relative foamability as a function of the scaled concentration, C/C_{50}, shown in Fig. 9. The obtained results show that in the intermediate concentration range around $C \sim C_{50}$ the experimental data group around the master curve independently of the method used for foam generation. At $C < C_{50}/10$ the relative foamability in FRM is significantly lower as compared to the relative foamability measured in the other three methods. To determine the reason for this effect, we calculated the threshold concentration required to ensure the formation of dense adsorption layer, C_A, on the bubble surface for a foam with volume equal to 50% of the maximum air that can be entrapped in the given method using the equation derived in Ref. [50]:

$$C_A = \frac{6\Phi\Gamma}{d_{32}(1-\Phi)} \quad (3)$$

Here Φ is the bubble volume fraction, Γ is the surfactant adsorption, and d_{32} is the mean volume-surface bubble diameter. To estimate C_A we assumed that $\Phi = V_{50\%}/(V_{50\%} + V_{sol})$, where $V_{50\%}$ is the half of the maximum volume of the air that can be entrapped under these conditions, $\Gamma = \Gamma_{TR}$ is given in Table 3 and $d_{32} \approx 1$ mm for the bubbles formed in BT and ST; $d_{32} = 500$ μm for bubbles formed in UT and FRM. The estimated values of C_A for the different methods are presented in Table 3.

The estimated values of C_A for PVA solutions are much higher as compared to those for low molecular mass surfactants, which is related to the much higher molecular mass of PVA. This comparison supports

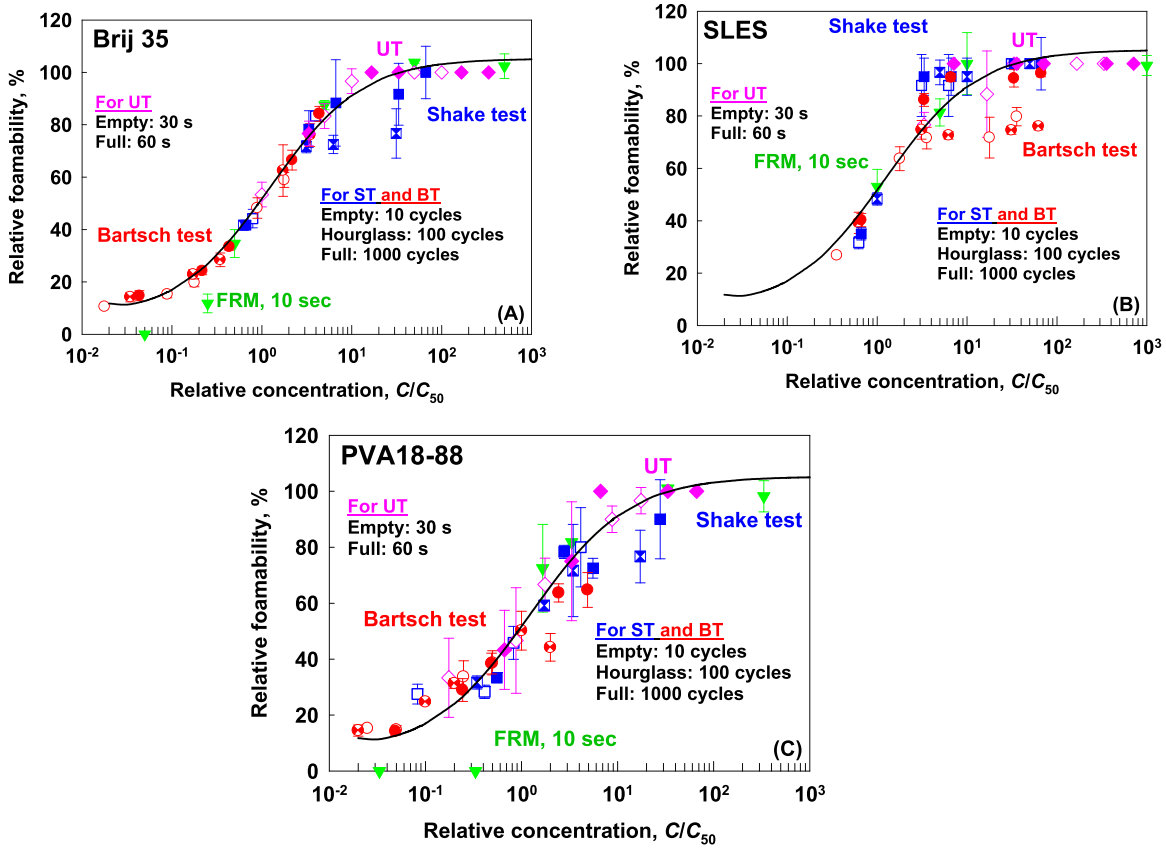

Fig. 9. Relative foamability as a function of scaled surfactant concentration C/C_{50} for (A) Brij 35; (B) SLES and (C) PVA 18–88. The curves are plotted according to Eq. (4).

the hypothesis that adsorption of lower molecular mass substances from PVA solutions occurs in the initial stage of bubble formation. The comparison of C_A for Brij 35 in the different methods shows that the values of $C_{50} >> C_A$ for Bartsch and shake tests, which means that the prevailing effect that controls the rate of foam generation in these two methods is the kinetics of adsorption on the bubble surface, whereas $C_{50} < C_A$ for foams formed in FRM which means that there is no enough surfactant to ensure bubble stabilization in this method at these very low concentrations. As a consequence, the foamability of the solutions in FRM decreases steeply with the decrease of bulk concentration and the respective results deviate from the master curve for Brij 35 and PVA 18–88. In the higher concentration range, the foamability in BT deviates from the master curve for SLES solutions at 10 shaking cycles. This deviation is related to the fact that additional increase in foam volume is observed for SLES in Bartsch at longer shaking cycles, see Fig. S8G.

It is seen that the shape of the relative foamability as a function of scaled concentration C/C_{50} is very similar for SLES, Brij 35 and PVA 18–88 in the different foaming tests. To check whether all obtained data in these tests can be represented by universal master curve we re-plotted the data shown in Fig. 7, S9, S10, S11 in the scale V/V_{max} vs C/C_{50}, see Fig. 10. All experimental data obtained in different methods, at different foaming times and with different foam stabilizers followed the same dependence well represented by sigmoidal equation:

$$V_A = V_{AMIN} + \frac{V_{AMAX} - V_{AMIN}}{1 + \exp\left(-\frac{(\lg(C/C_{50}) - b)}{d}\right)} \quad (4)$$

Here V_A is the volume of entrapped air; V_{AMAX} is the maximum air that can be entrapped in a given test; V_{AMIN} is the volume of air that is entrapped even at very low surfactant concentrations, C is the bulk concentration at which the test is performed, C_{50} is the threshold concentration required for entrapment of 50% of maximum foam volume in the test,and b and d are free adjustable parameters. From the best fit of all experimental data the adjustable parameters were determined as $V_{AMIN}/V_{AMAX} = 10.1\% \pm 1.6\%$; $b = 0.13 \pm 0.03$; $d = 0.44 \pm 0.02$. The regression coefficient is 0.95, which means that the proposed equation describes well the obtained experimental results in all studied tests with different surfactant and PVA solutions when $C_{50} > C_A$. When $C_{50} < C_A$, the foamability is controlled by the amount of surfactant that is present in the solution and could adsorb on the bubble surface during the foam generation, that is why, the data for FRM at low surfactant concentrations deviate from the general proposed dependence, Eq. (4).

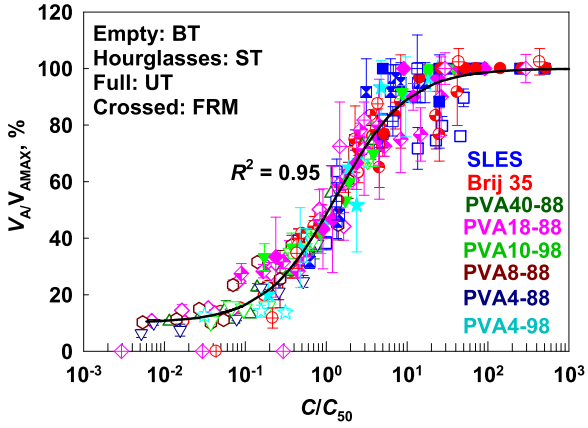

Fig. 10. Relative foamability, V_A/V_{AMAX}, as a function of the scaled concentration, C/C_{50}, for foams formed in four different foaming methods with different PVA and surfactant solutions. The continuous curve is calculated by Eq. (4) with $V_{AMIN}/V_{AMAX} = 10.1\% \pm 1.6\%$; $b = 0.13 \pm 0.03$; $d = 0.44 \pm 0.02$.

3.7. Relation between foam and surface properties

In our previous studies [15,16] we showed two master curves, one for anionic and one for nonionic surfactants, describe the foamability when plotted as a function of dynamic surface tension for foams prepared in Bartsch test. The initial tests show that in the new Bartsch test used in the current study, the appropriate time scale for obtaining the representative master curves is $t_u = 50$ ms. To test whether the previous observed dependences hold also for the polymeric solutions, we plotted the data from the foaming experiments shown in Fig. 6B as a function of the dynamic surface tension shown in Fig. 3B, see Fig. 11A. The results for V_A after 10 and 100 cycles as a function of DST at $t_u = 50$ ms are shown in Fig. S15. One sees that the results for PVA solutions lay between the data for the nonionic surfactant Brij 35 and the anionic surfactant SLES. The shape of the obtained curves for PVA resemble to some extend those for the nonionic surfactant, as expected, but show higher foamability at higher surface tension in comparison to Brij 35. From this plot we can conclude that the dynamic surface tension is not an appropriate parameter to interpret the data for polymeric solutions, because it depends very much on the presence of polymeric molecules with low molecular mass which adsorb faster on the bubble surface while being unable to ensure sufficient steric repulsion to prevent the bubble coalescence. That is why, at a given dynamic surface tension for PVA with 88% DH, the highest foamability is achieved when PVA with highest molecular mass is used (PVA 40–88) and the lowest foamability is determined when PVA 4–88 is used.

The experimental data for the dynamic surface tension were used to determine the instantaneous surface coverage during the foam generation by following the approach developed in Ref. [15]. The dependence of V_A vs $\Gamma(t_u = 50\text{ ms})/\Gamma_{TR}$ is shown in Fig. 11B. One sees that the data for different PVA solutions are grouped around a master line which is very close to the master curve for Brij 35, while the increase of foamability starts at surface coverage of 80% instead of 95% as in the case of Brij 35. Therefore, an intermediate behavior is observed with PVA solutions. The better foamability at the same surface coverage for PVA solutions (as compared to Brij 35) can be explained by the long-range steric repulsion between the PVA stabilized surfaces as seen from the images shown in Fig. 4. This long-range steric repulsion is less efficient, as compared to the electrostatic repulsion acting between SLES stabilized surfaces but it is more efficient when compared to the short-range steric repulsion acting between Brij 35 stabilized surfaces. The higher molecular mass of the polymer at given DH leads to formation of thicker foam films and lower dynamic surface coverage sufficient to boost the solution foamability as seen from the data shown in Fig. 11B.

4. Conclusions

Systematic series of experiments with one nonionic (Brij 35), one anionic (SLES) and 6 polyvinyl alcohol (PVA) solutions with two different degrees of hydrolysis (DH), 88% and 98%, and molecular weights (MW) varied between 27,000 and 205,000 g/mol are performed to compare their surface, film and foam properties. The foam properties are evaluated in four different foaming methods which differ in the rate of foam generation and in the way by which the gas is introduced in the solution, namely Bartsch test (fast foaming method), shake test and Ultra Turrax (foaming methods with intermediate rate of bubble expansion) and Foam rise method (slow foaming method with gas injection). The effect of surfactant and PVA concentration was also studied.

The dynamic and equilibrium surface tensions of PVA solutions strongly depend on the degree of PVA hydrolysis. The surface activity of PVA with 88% DH is much higher as compared to that of PVA with 98%. The average molecular mass of the polymers has almost no effect on the surface properties for samples with given DH. The foam films formed from PVA with 98% DH are unstable, whereas the film thickness and stability increase with increasing the MW for PVA with 88% DH due to the action of long range steric repulsion between the adsorbed polymeric

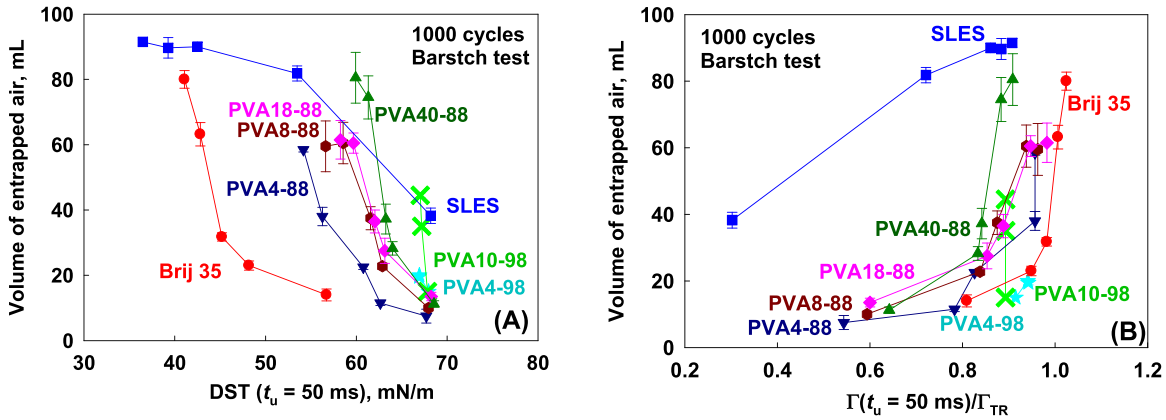

Fig. 11. Volume of entrapped air after 1000 shaking cycles in Bartsch test, as a function of (A) dynamic surface tension measured t_u = 50 ms in MBPM, and (B) dynamic surface coverage $\Gamma(t_u = 50\ ms)/\Gamma_{TR}$ for various surfactants and PVA samples. as indicated in the figures.

molecules on foam film surfaces.

The foamability increases with increasing the surfactant or polymer concentration in the solution for all used methods. The milder the conditions for gas entrapment, the lower concentration is required to prepare stable foams. The foamability in all foaming methods is the best for SLES, intermediate for Brij 35 and PVA with 88% DH, and the lowest for PVA with 98% DH. The concentration, C_{50}, required to entrap 50% of the maximum air in a given method decreases with increasing the number of shaking cycles in Bartsch test and the shake test, and with the stirring time in Ultra Turax. For a given surfactant, C_{50} is the lowest for the foam rise method, intermediate for shake test and Ultra Turrax, and the highest in Bartsch test. The value of C_{50} in a given method is the lowest for SLES, intermediate for Brij 35 and PVA with 88% DH, and the highest for PVA with 98% DH. The relative foamability for all studied surfactant and polymeric solutions followed the same master curve when plotted as a function of scaled surfactant concentration, C/C_{50}. Simple equation is proposed to describe the obtained experimental data for all studied surfactant and polymeric solutions in the different foaming methods, and at different times of foam generation. The deviations from this master curve at low surfactant concentrations for the foams formed in the FRM are explained with the insufficient amount of surface active molecules in the solution – they cannot cover the newly created bubble surface.

The foamability of PVA samples in different foaming methods can be explained under the assumption that these samples behave as nonionic surfactants and a threshold surface coverage is required for foam stabilization. However, this surface coverage (≈ 85%) is lower as compared to that for Brij 35 (≈ 95%). This difference is explained by the fact that a long-range steric repulsion acts between the foam film surfaces stabilized by PVA molecules. This long-range steric repulsion is more efficient to stabilize the foam films as compared to the short-range steric repulsion for Brij 35, while less efficient when compared to the electrostatic repulsion for SLES during the foam generation.

In the current study for first time it was shown that the approach developed in Ref. [15] for low molecular mass surfactants can be applied for foamability of PVA solutions. A new simple equation proposed in the current study for predicting the foamability is expected to be applicable for wide range of systems, although the characteristic times of each specific foam test could vary, depending on the test type and the specific hydrodynamic conditions (flow rate, rotation speed, frequency and amplitude of oscillations, etc.). One could expect future studies to expand and deepen this approach to a variety of other foam tests and surfactant systems.

Funding

This work was supported by Altana Institute, Germany and by Operational Program "Science and Education for Smart Growth" 2014–2020, co-funded by the European Union through the European Structural and Investment Funds, Grant BG05M2OP001–1.002–0012 "Sustainable utilization of bio-resources and waste of medicinal and aromatic plants for innovative bioactive products".

CRediT authorship contribution statement

Vassil Georgiev: Investigation, Formal analysis, Visualization, **Nikola Genchev:** Investigation; **Zlatina Mitrinova:** Formal analysis, Writing – Original draft. **Alexander Gers-Barlag**: Conceptualization; Funding acquisition; **Guillaume Jaunky:** Conceptualization; Funding acquisition. **Nikolai Denkov**: Conceptualization, Methodology, Funding acquisition. **Slavka Tcholakova**: Conceptualization, Methodology, Formal analysis, Writing – Review & Editing, Supervision.

Declaration of Competing Interest

The authors declare that they have no known competing financial interests or personal relationships that could have appeared to influence the work reported in this paper.

Data Availability

Data will be made available on request.

Appendix A. Supporting information

Supplementary data associated with this article can be found in the online version at doi:10.1016/j.colsurfa.2023.132828.

References

[1] S. Farrokhpay, The significance of froth stability in mineral flotation - a review, Adv. Colloid Interface Sci. 166 (2011) 1–7.
[2] A. Arzhavitina, H. Steckel, Foams for pharmaceutical and cosmetic application, Int. J. Pharm. 394 (2010) 1–17.
[3] R.J. Pugh, Foaming, foam films, antifoaming and defoaming, Adv. Colloid Interface Sci. 64 (1996) 67–142.
[4] D.L. Weaire, S. Hutzler, The Physics of Foams, Oxford University Press, Oxford, 2001.
[5] I. Cantat, S. Cohen-Addad, F. Elias, F. Graner, R. Höhler, O. Pitois, Foams: Structure and Dynamics. Oxford, Oxford University Press, 2013.
[6] J.J. Bikerman, Measurement of Foaminess. Foams, Springer-Verlag,, New York, 1973, pp. 65–97.
[7] E. Carey, C. Stubenrauch, Foaming properties of mixtures of a non-ionic (C12DMPO) and an ionic surfactant (C12TAB), J. Colloid Interface Sci. 346 (2010) 414–423.
[8] D. Kawale, A.T. van Nimwegen, L.M. Portela, M.A. van Dijk, R.A.W.M. Henkes, The relation between the dynamic surface tension and the foaming behaviour in a sparger setup, Colloids Surf. A. 336 (2015), 481328.

[9] N.D. Denkov, Mechanisms of foam destruction by oil-based antifoams, Langmuir 20 (2004) 9463–9505.
[10] D. Beneventi, B. Carre, A. Gandini, Role of surfactant structure on surface and foaming properties, Colloids Surf. A 189 (1–3) (2001) 65–73.
[11] C.D. Dushkin, T.L. Stoichev, T.S. Horozov, A. Mehreteab, G. Broze, Dynamics of foams of ethoxylated ionic surfactant in the presence of micelles and multivalent ions, Colloid Polym. Sci. 281 (2) (2003) 130–142.
[12] A.K.S. Chesterton, G.D. Moggridge, P.A. Sadd, D.I. Wilson, Modelling of shear rate distribution in two planetary mixtures for studying development of cake batter structure, J. Food Eng. 105 (2) (2011) 343–350.
[13] I. Lesov, S. Tcholakova, N. Denkov, Factors controlling the formation and stability of foams used as precursors of porous materials, J. Colloid Interface Sci. 426 (2014) 9–21.
[14] N. Politova, S. Tcholakova, Z. Valkova, K. Golemanov, N.D. Denkov, Self-regulation of foam volume and bubble size during foaming via shear mixing, Colloids Surf. A 539 (2018) 18–28.
[15] B. Petkova, S. Tcholakova, M. Chenkova, K. Golemanov, N. Denkov, D. Thorley, S. Stoyanov, Foamability of aqueous solutions: role of surfactant type and concentration, Adv. Colloid Interface Sci. 276 (2020), 102084.
[16] B. Petkova, S. Tcholakova, N. Denkov, Foamability of Surfactant Solutions: Interplay Between Adsorption and Hydrodynamic Conditions, Colloids Surf. A 626 (2021), 127009.
[17] R. Singh, K.K. Mohanty, A simple, efficient, and eco-friendly method for the preparation of 3-substituted-2,3-dihydroquinazolin-4(1H)-one derivatives, Molecules 24 (2019).
[18] O. Bartsch, Über Schaumsysteme, Kolloidchem. Beih. 20 (1–5) (1924) 1–49.
[19] J. Lee, A. Nikolov, D. Wasan, Effects of micellar structuring and solubilized oil on the kinetic stability of aqueous foams, Ind. Eng. Chem. Res. 53 (49) (2014) 18891–18899.
[20] N.D. Denkov, K.G. Marinova, S.S. Tcholakova, Mechanistic understanding of the modes of action of foam control agents, Adv. Colloid Interface Sci. 206 (2014) 57–67.
[21] M.J. Rosen, J. Solash, Factors affecting initial foam height in the Ross-Miles foam test, J. Am. Oil Chem. Soc. 46 (8) (1969) 399–402.
[22] S. Samanta, P. Ghosh, Coalescence of bubbles and stability of foams in aqueous solutions of Tween surfactants, Chem. Eng. Res. Des. 89 (11) (2011) 2344–2355.
[23] H. Azira, A. Tazerouti, J.P. Canselier, Study of foaming properties and effect of the iomeric distribution of some anionic surfactants, J. Surfactants Deterg. 11 (4) (2008) 279–286.
[24] N. Denkov, S. Tcholakova, N. Politova-Brinkova, Physicochemical Control of Foam Properties, Curr. Opin. Colloid Interface Sci. 50 (2020), 101376.
[25] D.J.F. Taylor, R.K. Thomas, J. Penfold, Polymer/surfactant interactions at the air/water interface, Adv. Colloid Interface Sci. 132 (2) (2007) 69–110.
[26] D. Langevin, Polyelectrolyte and surfactant mixed solutions. Behavior at surfaces and in thin films, Adv. Colloid Interface Sci. 89–90 (2001) 467–484.
[27] N. Kristen, R. von Klitzing, Effect of polyelectrolyte/surfactant combinations on the stability of foam films, Soft Matter 6 (2010) 849.
[28] C. Uzum, N. Kristen, R. von Klitzing, Polyelectrolytes in thin liquid films, Curr. Opin. Colloid Int. Sci. 15 (2010) 303.
[29] A. Bhattacharyya, F. Monroy, D. Langevin, J.F. Argillier, Surface rheology and foam stability of mixed surfactant–polyelectrolyte solutions, Langmuir 16 (2000) 8727.
[30] R. Petkova, S. Tcholakova, N. Denkov, Foaming and foam stability for mixed polymer−surfactant solutions: Effects of surfactant type and polymer charge, Langmuir 28 (2012) 4996–5009.
[31] B.M. Folmer, B. Kronberg, Effect of surfactant–polymer association on the stabilities of foams and thin films: sodium dodecyl sulphate and poly(vinyl pyrrolidone), Langmuir 16 (2000) 5987.
[32] A. Cervantes-Martinez, A. Maldonado, Foaming behaviour of polymer–surfactant solutions, J. Phys. Condens Matter 19 (2007), 246101.
[33] R. Nagarkar, J. Patel, Polyvinyl Alcohol: A Comprehensive Study, Acta Sci. Pharm. Sci. 3 (4) (2019) 34–44.
[34] Q. Hou, X. Wang, The effect of PVA foaming characteristics on foam forming, Cellulose 24 (2017) 4939–4948.
[35] P.A. Kralchevsky, K.D. Danov, N.D. Denkov, Chemical physics of colloid systems and interfaces., editor. Chapter 7 in, in: K.S. Birdi (Ed.), Handbook of Surface and Colloid Chemistry, 3rd updated ed., CRC Press, Boca Raton, FL, 2008.
[36] N.C. Christov, K.D. Danov, P.A. Kralchevsky, K.P. Ananthapadmanabhan, A. Lips, Maximum bubble pressure method: universal surface age and transport mechanisms in surfactant solutions, Langmuir 22 (2006) 7528–7542.
[37] A. Scheludko, Thin liquid films, Adv. Colloid Interface Sci. 1 (1967) 391–464.
[38] K. Golemanov, N.D. Denkov, S. Tcholakova, M. Vethamuthu, A. Lips, Surfactant Mixtures for Control of Bubble Surface Mobility in Foam Studies, Langmuir 24 (2008) 9956–9961.
[39] J. Zhang, R.K. Thomas, J. Penfold, Collapsed Structure of Hydrophobically Modified Polyacrylamide Adsorbed at the Air−Water Interface: The Polymer Surface Excess and the Gibbs Equation, Langmuir 36 (2020) 11661–11675.
[40] S.W. An, R.K. Thomas, C. Forder, N.C. Billingham, S.P. Armes, J. Penfold, Behavior of Nonionic Water Soluble Homopolymers at the Air/Water Interface: Neutron Reflectivity and Surface Tension Results for Poly(vinyl methyl ether), Langmuir 18 (13) (2002) 5064–5073.
[41] J.A. De Feijter, J. Benjamins, Adsorption behavior of pva at the air—water interface. I. Applicability of the gibbs adsorption equation, J. Colloid Interface Sci. 81 (1) (1981) 91–107.
[42] R. Olayo, E. Garcia, B. 1 Garcia-Corichi, L. Sanchez-Vazquez, J. Alvarez, Poly(vinyl alcohol) as a Stabilizer in the Suspension Polymerization of Styrene: The Effect of the Molecular Weight, J. Appl. Polym. Sci. 67 (1998) 71–77.
[43] T. Shiomi, T. Tsuchida, K. Imai, Surface tension of aqueous solutions of poly(vinyl alcohol) with pendant alkyl groups, J. Colloid Interface Sci. 99 (2) (1984) 586–587.
[44] P. Linse, T.A. Hatton, Mean-Field Lattice Calculations of Ethylene Oxide and Propylene Oxide Containing Homopolymers and Triblock Copolymers at the Air/Water Interface, Langmuir 13 (15) (1997) 4066–4078.
[45] S. Khosharay, M. Rahmanzadeh, B. ZareNezhad, Surface Behavior of Aqueous Solutions of Sodium Lauryl Ether Sulfate, Additives and Their Mixtures: Experimental and Modeling Study, Int J. Thermophys. 41 (2020), 166.
[46] H. Xu, P. Li, K. Ma, R.K. Thomas, J. Penfold, J.R. Lu, Limitations in the Application of the Gibbs Equation to Anionic Surfactants at the Air/Water Surface: Sodium Dodecylsulfate and Sodium Dodecylmonooxyethylenesulfate Above and Below the CMC, Langmuir 29 (30) (2013) 9335–9351.
[47] N.C. Christov, K.D. Danov, P.A. Kralchevsky, K.P. Ananthapadmanabhan, A. Lips, Maximum bubble pressure method: universal surface age and transport mechanisms in surfactant solutions, Langmuir 22 (2006) 7528–7542.
[48] O. Squillace, R. Fong, O. Shepherd, J. Hind, J. Tellam, N.-J. Steinke, R. L. Thompson, Influence of PVAc/PVA Hydrolysis on Additive Surface Activity, Polymers 12 (2020) 205.
[49] S. Chibowski, M. Paszkiewicz, M. Wiśniewska, The Influence of Surfactant (SDS) on the Adsorption Properties of Polyvinyl S Alcohol and Polyethylene Glycol in an Alumina/Solution System, Adsorpt. Sci. Technol. 20 (2002) 6.
[50] S. Tcholakova, N.D. Denkov, D. Sidzhakova, I.B. Ivanov, B. Campbell, Interrelation between Drop Size and Protein Adsorption at Various Emulsification Conditions, Langmuir 19 (14) (2003) 5640–5649.